

Probing the QCD pomeron in doubly tagged e^+e^- collisions

J. KWIECIŃSKI^a, L. MOTYKA^b

^a*Department of Theoretical Physics,*

H. Niewodniczański Institute of Nuclear Physics, Cracow, Poland

^b*Institute of Physics, Jagellonian University, Cracow, Poland*

Abstract

We calculate the total cross-section for $\gamma^*\gamma^*$ collisions and for the process $e^+e^- \rightarrow e^+e^- + \text{hadrons}$ with two tagged leptons assuming dominance of the QCD pomeron exchange. We solve the BFKL equation including the dominant subleading effects generated by the consistency constraint which restricts the available phase-space of the emitted gluons to the region in which the virtuality of the exchanged gluons is dominated by their transverse momentum squared. Estimate of the possible soft pomeron contribution to the $\gamma^*\gamma^*$ cross-section is also presented. At very high CM energies W the calculated total $\gamma^*\gamma^*$ cross-section exhibits effective power-law $(W^2)^\lambda$ behaviour with $\lambda \sim 0.3$. We confront our results with the recent measurements at LEP and give predictions for the energies which can be accessible at TESLA and at other future linear e^+e^- colliders.

It has been pointed out [1, 2, 3] that the measurement of the cross section of the doubly tagged process $e^+e^- \rightarrow e^+e^- + \text{hadrons}$, which is controlled by the total cross-section describing the interaction of two virtual photons, i.e. the process $\gamma^*\gamma^* \rightarrow \text{hadrons}$ can be a very useful tool for probing the QCD pomeron (see Fig. 1). In the leading logarithmic approximation the QCD pomeron corresponds to the sum of ladder diagrams with reggeized gluons along the chain. This sum is described by the Balitzkij, Fadin, Kuraev, Lipatov (BFKL) equation [4, 5].

Important property of the process $\gamma^*\gamma^* \rightarrow \text{hadrons}$ is the fact that by a suitable choice of the kinematical cuts one can select the configuration in which $Q_1^2 \sim Q_2^2$ with both Q_i^2 being large. In this kinematical configuration, when the two relevant scales are comparable the conventional LO QCD evolution from the scale Q_1^2 to Q_2^2 is suppressed and one can expect that the potential increase of the total cross-section with energy would then be sensitive to the diffusion of transverse momenta within the gluon ladder which generates the QCD pomeron. The process $\gamma^*\gamma^* \rightarrow \text{hadrons}$ has also the advantage that for large Q_i^2 its cross-section can be entirely calculated perturbatively.

Existing estimates of the total cross-sections of the process $\gamma^*\gamma^* \rightarrow \text{hadrons}$ have been performed within the leading logarithmic approximation of the QCD pomeron. It has however been found recently that the BFKL equation which generates the QCD pomeron can acquire very significant non-leading corrections [6, 7]. The purpose of this paper is therefore to (re-) analyse the total $\gamma^*\gamma^*$ cross-section taking the subleading BFKL effects into account. To be precise we shall base our calculations on the (modified) BFKL equation with the consistency constraint limiting the phase space of the real gluon emission. This constraint is based on the requirement that the virtuality of the exchanged gluons is dominated by their transverse momentum squared. Let us remind that the form of the LO BFKL kernel where the gluon propagators contain only the gluon transverse momentum squared etc. is only valid within the region of phase space restricted by this constraint. Formally however, the consistency constraint generates subleading corrections. It can be shown that at the NLO accuracy it generates about 70% of the exact result for the QCD pomeron intercept. Very important merit of this constraint is the fact that it automatically generates resummation of higher order contributions which stabilizes the solution [8].

The cross-section of the process $e^+e^- \rightarrow e^+e^- + \text{hadrons}$ (averaged over the angle ϕ between the lepton scattering planes in the frame in which the virtual photons are aligned

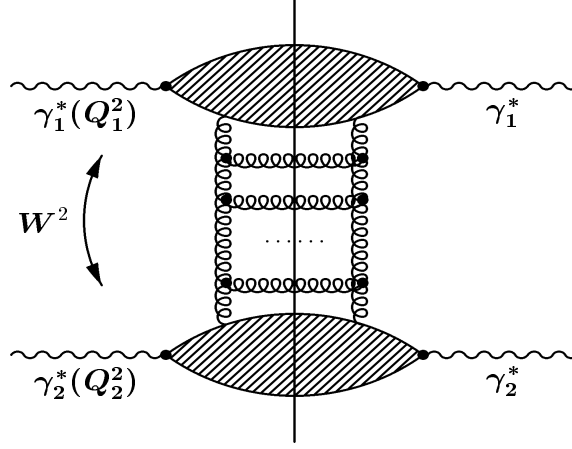


Figure 1: The QCD pomeron exchange mechanism of the process $\gamma_1^*(Q_1^2)\gamma_2^*(Q_2^2) \rightarrow \text{hadrons}$.

along the z axis) is given by the following formula [1]:

$$\begin{aligned} \frac{Q_1^2 Q_2^2 d\sigma}{dy_1 dy_2 dQ_1^2 dQ_2^2} = & \left(\frac{\alpha}{2\pi}\right)^2 [P_{\gamma/e^+}^{(T)}(y_1)P_{\gamma/e^-}^{(T)}(y_2)\sigma_{\gamma^*\gamma^*}^{TT}(Q_1^2, Q_2^2, W^2) + \\ & P_{\gamma/e^+}^{(T)}(y_1)P_{\gamma/e^-}^{(L)}(y_2)\sigma_{\gamma^*\gamma^*}^{TL}(Q_1^2, Q_2^2, W^2) + \\ & P_{\gamma/e^+}^{(L)}(y_1)P_{\gamma/e^-}^{(L)}(y_2)\sigma_{\gamma^*\gamma^*}^{LL}(Q_1^2, Q_2^2, W^2)] \end{aligned} \quad (1)$$

where

$$P_{\gamma/e}^{(T)}(y) = \frac{1 + (1 - y)^2}{y} \quad (2)$$

$$P_{\gamma/e}^{(L)}(y) = 2\frac{1 - y}{y} \quad (3)$$

In Eq. (1) y_1 and y_2 are the longitudinal momentum fractions of the parent leptons carried by virtual photons, $Q_i^2 = -q_i^2$ ($i = 1, 2$) where $q_{1,2}$ denote the four momenta of the virtual photons and W^2 is the total CM energy squared of the two (virtual) photon system, i.e. $W^2 = (q_1 + q_2)^2$. The cross-sections $\sigma_{\gamma^*\gamma^*}^{ij}(Q_1^2, Q_2^2, W^2)$ are the total cross-sections of the process $\gamma^*\gamma^* \rightarrow \text{hadrons}$ and the indices $i, j = T, L$ denote the polarization of the virtual photons. The functions $P_{\gamma/e}^{(T)}(y)$ and $P_{\gamma/e}^{(L)}(y)$ are the transverse and longitudinal photon flux factors.

The cross-sections $\sigma_{\gamma^*\gamma^*}^{ij}(Q_1^2, Q_2^2, W^2)$ are given by the following formula:

$$\begin{aligned} \sigma_{\gamma^*\gamma^*}^{ij}(Q_1^2, Q_2^2, W^2) = & P_S(Q_1^2, Q_2^2, W^2)\delta_{iT}\delta_{jT} + \\ & \frac{1}{2\pi} \sum_q \int_{k_0^2}^{k_{max}^2(Q_2^2, x)} \frac{dk^2}{k^4} \int_{\xi_{min}(k^2, Q_2^2)}^{1/x} d\xi G_q^{0j}(k^2, Q_2^2, \xi) \Phi_i(k^2, Q_1^2, x\xi) \end{aligned} \quad (4)$$

where

$$k_{max}^2(Q_2^2, x) = -4m_q^2 + Q_2^2 \left(\frac{1}{x} - 1 \right) \quad (5)$$

$$\xi_{min}(k^2, Q^2) = 1 + \frac{k^2 + 4m_q^2}{Q^2} \quad (6)$$

and

$$x = \frac{Q_2^2}{2q_1q_2} \quad (7)$$

The functions $G_q^{0i}(k^2, Q^2, \xi)$, which describe the coupling of the two gluon system to virtual photons corresponding to the quark box and crossed-box diagrams are defined as below [1, 9]

$$\begin{aligned} G_q^{0T}(k^2, Q^2, \xi) = & \\ & 2\alpha_{em}\alpha_s(k^2 + m_q^2)e_q^2 \int_0^{\rho_{max}} d\rho \int \frac{d^2p'}{\pi} \delta \left[\xi - \left(1 + \frac{p'^2 + m_q^2}{z(1-z)Q^2} + \frac{k^2}{Q^2} \right) \right] \times \\ & \left\{ \left[(z^2 + (1-z)^2) \left(\frac{\mathbf{p}}{D_1} - \frac{\mathbf{p}+\mathbf{k}}{D_2} \right)^2 \right] + m_q^2 \left(\frac{1}{D_1} - \frac{1}{D_2} \right)^2 \right\} \end{aligned} \quad (8)$$

$$\begin{aligned} G_q^{0L}(k^2, Q^2, \xi) = & \\ & 8\alpha_{em}\alpha_s(k^2 + m_q^2)e_q^2 \int_0^{\rho_{max}} d\rho \int \frac{d^2p'}{\pi} \delta \left[\xi - \left(1 + \frac{p'^2 + m_q^2}{z(1-z)Q^2} + \frac{k^2}{Q^2} \right) \right] \times \\ & \left[z^2(1-z)^2 \left(\frac{1}{D_1} - \frac{1}{D_2} \right)^2 \right] \end{aligned} \quad (9)$$

where

$$z = \frac{1+\rho}{2} \quad (10)$$

$$\mathbf{p} = \mathbf{p}' + (z-1)\mathbf{k} \quad (11)$$

$$D_1 = p^2 + z(1-z)Q^2 + m_q^2$$

$$D_2 = (p+k)^2 + z(1-z)Q^2 + m_q^2 \quad (12)$$

$$\rho_{max} = \sqrt{1 - \frac{4m_q^2}{1/x - k^2/Q^2 - 1}} \quad (13)$$

with m_q denoting the quark mass. In our calculations we include contributions from u , d , s and c quarks and set $m_u = m_d = m_s = 0$ and $m_c = 1.5$ GeV.

The function $P_S(Q_1^2, Q_2^2, W^2)$ corresponds to the the contribution from the region $k^2 \leq k_0^2$ in the corresponding integrals over the gluon transverse momenta. It is assumed to

be dominated by the soft pomeron contribution which is estimated from the factorisation of its couplings, i.e.

$$P_S(Q_1^2, Q_2^2, W^2) = \frac{\sigma_{\gamma^*(Q_1^2)p}^{SP}(Q_1^2, W^2)\sigma_{\gamma^*(Q_2^2)p}^{SP}(Q_2^2, W^2)}{\sigma_{pp}^{SP}(W^2)} \quad (14)$$

We assume that this term is only contributing to the transverse part. In equation (14) the cross-sections $\sigma_{\gamma^*(Q_i^2)p}^{SP}(Q_i^2, W^2)$ and $\sigma_{pp}^{SP}(W^2)$ are the soft pomeron contributions to the γ^*p and pp total cross sections and their parametrisation is taken from Refs. [10, 11]. Their W^2 dependence is, of course, universal i.e.

$$\begin{aligned} \sigma_{pp}^{SP}(W^2) &= \beta_p^2 \left(\frac{W^2}{W_0^2} \right)^{\alpha_{SP}(0)-1} \\ \sigma_{\gamma^*(Q^2)p}^{SP}(Q^2, W^2) &= \beta_{\gamma^*}(Q^2)\beta_p \left(\frac{W^2}{W_0^2} \right)^{\alpha_{SP}(0)-1} \end{aligned} \quad (15)$$

with $W_0 = 1$ GeV and $\alpha_{SP}(0) \approx 1.08$.

The function $\beta_{\gamma^*}(Q^2)$ behaves for large Q^2 as $\beta_{\gamma^*}(Q^2) \sim (Q^2)^{-\alpha_{SP}(0)}$ and so the factorisation formula (14) implies that the soft pomeron contribution to the total $\gamma^*\gamma^*$ cross-section should behave as:

$$P_S(Q_1^2, Q_2^2, W^2) \sim \left(\frac{W^2 W_0^2}{Q_1^2 Q_2^2} \right)^{\alpha_{SP}(0)-1} \frac{1}{Q_1^2 Q_2^2} \quad (16)$$

The functions $\Phi_i(k^2, Q^2, x_g)$ in the second term in Eq. (4) satisfy the Balitzkij, Fadin, Kuraev, Lipatov (BFKL) equation which, in the leading $\ln(1/x)$ approximation have the following form:

$$\begin{aligned} \Phi_i(k^2, Q^2, x_g) &= \Phi_i^0(k^2, Q^2, x_g) + \Phi^S(k^2, Q^2, x_g)\delta_{iT} + \frac{3\alpha_s(k^2)}{\pi}k^2 \int_{x_g}^1 \frac{dx'}{x'} \int_{k_0^2}^\infty \frac{dk'^2}{k'^2} \\ &\quad \left[\frac{\Phi_i(k'^2, Q^2, x') - \Phi_i(k^2, Q^2, x')}{|k'^2 - k^2|} + \frac{\Phi_i(k^2, Q^2, x')}{\sqrt{4k'^4 + k^4}} \right] \end{aligned} \quad (17)$$

The term proportional to the function $\Phi_i(k'^2, Q^2, x')$ under the integral corresponds to the real gluon emission while the terms proportional to $\Phi_i(k^2, Q^2, x')$ to virtual corrections which are responsible for gluon reggeisation. The inhomogeneous terms $\Phi_i^0(k^2, Q^2, x_g)$ and $\Phi^S(k^2, Q^2, x_g)$ will be defined later.

In the small x_g limit the solution of the BFKL equation (17) behaves as

$$\Phi_i(k^2, Q^2, x_g) \sim x_g^{-\lambda_{QCD}} \quad (18)$$

If in equation (17) the running QCD coupling $\alpha_s(k^2)$ is replaced by the fixed (i.e. k^2 independent) coupling $\tilde{\alpha}_s$ then the exponent λ_{QCD} is given by the following formula [4]:

$$\lambda_{QCD} = \frac{6\tilde{\alpha}_s}{\pi}[\psi(1) - \psi(1/2)] \quad (19)$$

with $\psi(z) = \Gamma'(z)/\Gamma(z)$, where $\Gamma(z)$ is the Euler Gamma function and $2[\psi(1) - \psi(1/2)] = 4 \ln 2$. The quantity $1 + \lambda_{QCD}$ is the QCD pomeron intercept.

In what follows we shall consider the modified BFKL equation in which we restrict the available phase-space in the real gluon emission by the consistency constraint:

$$k'^2 \leq k^2 \frac{x'}{x_g} \quad (20)$$

This constraint follows from the requirement that the virtuality of the exchanged gluons is dominated by their transverse momentum squared. Modified BFKL equations take the following form:

$$\begin{aligned} \Phi_i(k^2, Q^2, x_g) = & \Phi_i^0(k^2, Q^2, x_g) + \Phi^S(k^2, Q^2, x_g)\delta_{iT} + \frac{3\alpha_s(k^2)}{\pi}k^2 \int_{x_g}^1 \frac{dx'}{x'} \int_{k_0^2}^{\infty} \frac{dk'^2}{k'^2} \\ & \left[\frac{\Phi_i(k'^2, Q^2, x')\Theta\left(k^2 \frac{x'}{x_g} - k'^2\right) - \Phi_i(k^2, Q^2, x')}{|k'^2 - k^2|} + \frac{\Phi_i(k^2, Q^2, x')}{\sqrt{4k'^4 + k^4}} \right] \end{aligned} \quad (21)$$

The consistency constraint (20) lowers the QCD pomeron intercept since the exponent λ_{QCD} can be shown to be now the solution of the following equation (for the fixed coupling $\tilde{\alpha}_s$):

$$\lambda_{QCD} = \frac{6\tilde{\alpha}_s}{\pi} \left[\psi(1) - \psi\left(\frac{1 + \lambda_{QCD}}{2}\right) \right] \quad (22)$$

This equation introduces subleading corrections to the QCD pomeron intercept and generates their (approximate) resummation to all orders. In the next-to-leading approximation it exhausts about 3/4 of the entire next-to-leading contribution to λ_{QCD} . Another feature of the modified BFKL equation (21) is the delay of the onset of the power-law behaviour (18) (with λ_{QCD} defined now by Eq. (22)) to smaller values of x_g than in the case of the leading order approximation. This is caused by the fact that for moderately small values of x_g the (negative) virtual contribution to the BFKL equation, which is unaffected by the consistency constraint, dominates over the positive real emission term constrained by the Theta function in Eq. (21). Both effects (i.e. lowering of the intercept and delay of the onset of asymptotic small x_g behaviour) substantially reduce the corresponding cross-section. In what follows we shall numerically solve equation (21) with the running coupling constant $\alpha_s(k^2)$.

The inhomogeneous terms in equations (17,21) are the sum of two contributions $\Phi_i^0(k^2, Q^2, x_g)$ and $\Phi^S(k^2, Q^2, x_g)\delta_{iT}$. The first contributions ($\Phi_i^0(k^2, Q^2, x_g)$) correspond to the diagrams in which the two gluon system couples to virtual photons through a quark box and are given by following equations:

$$\Phi_i^0(k^2, Q^2, x_g) = \sum_q \int_{x_g}^1 dz \tilde{G}_{iq}^0(k^2, Q^2, z) \quad (23)$$

where

$$\begin{aligned} \tilde{G}_{Tq}^0(k^2, Q^2, z) = 2\alpha_{em}e_q^2\alpha_s(k^2 + m_q^2) \int_0^1 d\lambda \left\{ \frac{[\lambda^2 + (1-\lambda)^2][z^2 + (1-z)^2]k^2}{\lambda(1-\lambda)k^2 + z(1-z)Q^2 + m_q^2} + \right. \\ \left. 2m_q^2 \left[\frac{1}{z(1-z)Q^2 + m_q^2} - \frac{1}{\lambda(1-\lambda)k^2 + z(1-z)Q^2 + m_q^2} \right] \right\} \end{aligned} \quad (24)$$

$$\begin{aligned} \tilde{G}_{Lq}^0(k^2, Q^2, z) = 16\alpha_{em}Q^2k^2e_q^2\alpha_s(k^2 + m_q^2) \times \\ \int_0^1 d\lambda \left\{ \frac{[\lambda(1-\lambda)][z^2(1-z)^2]}{[\lambda(1-\lambda)k^2 + z(1-z)Q^2 + m_q^2][z(1-z)Q^2 + m_q^2]} \right\} \end{aligned} \quad (25)$$

The functions $\tilde{G}_{iq}^0(k^2, Q^2, z)$ are obtained from $G_q^{0i}(k^2, Q^2, \xi)$ after integrating over $d\xi$ and unfolding integration over $d\rho$ in equations (8) and (9). The second term $\Phi^S(k^2, Q^2, x_g)\delta_{iT}$, which is assumed to contribute only to the transverse component corresponds to the contribution to the BFKL equation from the non-perturbative soft region $k'^2 < k_0^2$. Adopting the strong ordering approximation $k'^2 \ll k^2$ it is given by the following formula:

$$\Phi^S(k^2, Q^2, x_g) = \frac{3\alpha_s(k^2)}{\pi} \int_{x_g}^1 \frac{dx'}{x'} \int_0^{k_0^2} \frac{dk'^2}{k'^2} \Phi_T(k'^2, Q^2, x') \quad (26)$$

The last integral in equation (26) can be interpreted as a gluon distribution in a virtual photon of virtuality Q^2 evaluated at the scale k_0^2 . At low values of x' it is assumed to be dominated by a soft pomeron contribution and can be estimated using the factorisation of the soft pomeron couplings:

$$\int_0^{k_0^2} \frac{dk'^2}{k'^2} \Phi_T(k'^2, Q^2, x') = \pi^2 x' g_p(x', k_0^2) \frac{\beta_{\gamma^*}(Q^2)}{\beta_p} \quad (27)$$

where $g_p(x', k_0^2)$ is the gluon distribution in a proton at the scale k_0^2 and the couplings $\beta_{\gamma^*}(Q^2)$ and β_p defined by equation (15).

In Fig. 2a we show our results for $\sigma_{\gamma^*\gamma^*}^{TT}(Q_1^2, Q_2^2, W^2)$ plotted as the function of the CM energy W for three different values of Q^2 where $Q_1^2 = Q_2^2 = Q^2$. We plot in this figure:

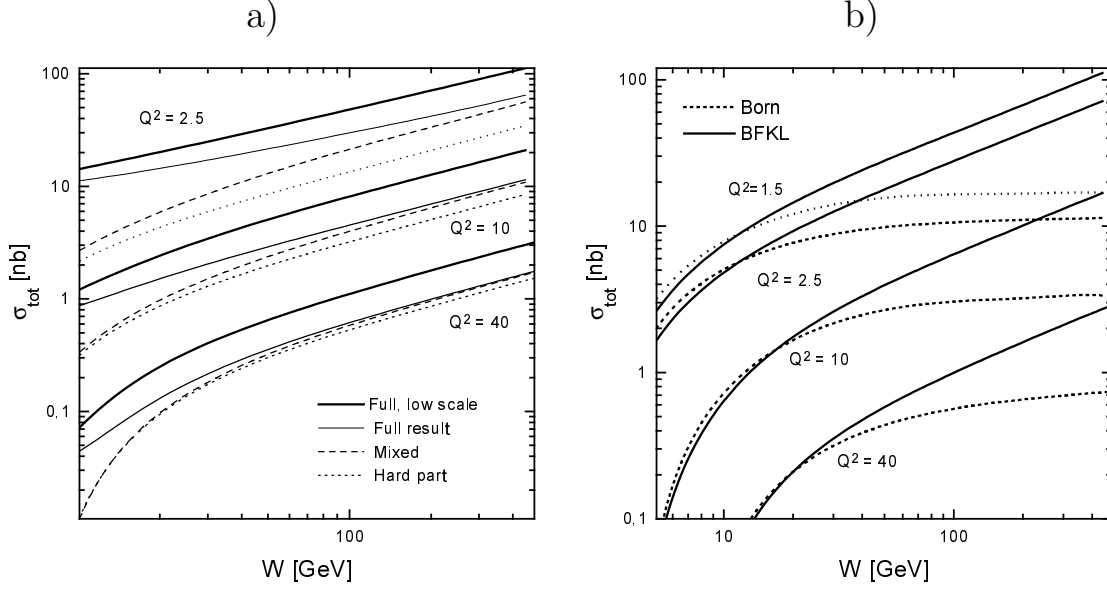


Figure 2: Energy dependence of the cross-section $\sigma_{\gamma^*\gamma^*}^{TT}(Q_1^2, Q_2^2, W^2)$ for the process $\gamma^*(Q_1^2)\gamma^*(Q_2^2) \rightarrow \text{hadrons}$ for various choices of photon virtualities $Q^2 = Q_1^2 = Q_2^2$: a) Complete i.e. including soft and QCD pomeron contributions results corresponding to Eq. (4). For each choice of the virtuality Q^2 four curves are shown taking into account hard effects only (“hard part”), hard amplitude with soft pomeron contributions added in the source term of the BFKL equation (“mixed”), the full cross-section including both soft and hard pomeron contributions (“full result”). We also show the “full result” with the low scale of α_s in the impact factors: $\mu^2 = (k^2 + m_q^2)/4$. b) Comparison of the complete contribution of the perturbative QCD pomeron to the cross-section $\sigma_{\gamma^*\gamma^*}^{TT}(Q^2, Q^2, W^2)$ (continuous line) with its Born term component corresponding to the two gluon exchange mechanism (dotted line).

1. the pure perturbative QCD (i.e. “hard”) contribution obtained from solving the BFKL equation with the consistency constraint included (see Eq. (21)) and with the inhomogeneous term containing only the QCD impact factor defined by equations (23,24,25);
2. the “mixed” contribution generated by the BFKL equation (21) with the soft pomeron contribution defined by equations (26, 27) included in the inhomogeneous term;
3. The “full” contribution which also contains the soft pomeron term (14).

We also show results obtained by changing the scale of the strong coupling α_s in the impact factors from $k^2 + m_q^2$ to $(k^2 + m_q^2)/4$. The scale of α_s in the BFKL equation was

set equal to k^2 in both the cases.

We see from this figure that the effects of the soft pomeron contribution are non-negligible at low and moderately large values of $Q^2 < 10 \text{ GeV}^2$ and for moderately large values of $W < 100 \text{ GeV}$. The QCD pomeron however dominates already at $Q^2 = 40 \text{ GeV}^2$. We also see from this figure that for low energies $W < 40 \text{ GeV}$ the phase-space limitations (cf. Eqs. (5) and (6)) are very important. For $W > 40 \text{ GeV}$ or so one observes that the cross-section exhibits the effective power-law behaviour $\sigma_{\gamma^*\gamma^*}^{TT}(Q^2, Q^2, W^2) \sim (W^2)^\lambda$. The (effective) exponent increases weakly with increasing Q^2 and varies from $\lambda = 0.28$ for $Q^2 = 2.5 \text{ GeV}^2$ to $\lambda = 0.33$ for $Q^2 = 40 \text{ GeV}^2$. This (weak) dependence of the effective exponent λ on Q^2 is the result of the interplay between soft and hard pomeron contributions, where the former becomes less important at large Q^2 . The shape of the remaining cross sections $\sigma_{\gamma^*\gamma^*}^{TL}$, $\sigma_{\gamma^*\gamma^*}^{LT}$ and $\sigma_{\gamma^*\gamma^*}^{LL}$ as functions of W is the same as that of $\sigma_{\gamma^*\gamma^*}^{TT}$. They do however differ in their relative normalisation.

In Fig. 2b we compare the QCD pomeron contribution to the cross-section $\sigma_{\gamma^*\gamma^*}^{TT}$ with the Born term, which corresponds to the two-gluon exchange mechanism. The latter contribution is given by equation (4) with the functions $\Phi_i(k^2, Q_1^2, x\xi)$ approximated by the impact factors $\Phi_i^0(k^2, Q_1^2, x\xi)$ defined by equations (23), (24) and (25). For large values of the CM energy W the two-gluon exchange mechanism gives energy independent contribution to the cross-section $\sigma_{\gamma^*\gamma^*}^{TT}$. In the low energy region its energy dependence (i.e. the onset of the constant asymptotic behaviour) is controlled by phase space effects embodied in equations (4), (5) and (6). We can also see from this figure that the dominance of the BFKL pomeron over its Born term is delayed to higher energies. In the low energy region the cross-section corresponding to the solution of the modified BFKL equation (21) is even smaller than that which is given by the Born term. This is caused by the fact, which we have already mentioned above, that for moderately small values of x_g/x' the consistency constraint (20) suppresses the (positive) real emission contribution to the BFKL kernel while leaving unaffected the (negative) virtual corection term (cf. Eq. (21)).

We have also calculated the total cross-section of the process $e^+e^- \rightarrow e^+e^- + \text{hadrons}$ (see Eq. (1)) for LEP1 and LEP2 energies and confronted results of our calculation with the recent experimental data obtained by the L3 collaboration at LEP [12]. Comparison of our results with experimental data is summarised in Tab. 1. We show comparison for $d\sigma/dY$, where $Y = \ln(W^2/Q_1Q_2)$ with subtracted Quark Parton Model (QPM) contribu-

ΔY	$\langle d\sigma/dY \rangle$ [fb]					
	Data — QPM	Theory (BFKL+SP)				
		$\alpha_s[(k^2 + m_q^2)/4]$			$\alpha_s(k^2 + m_q^2)$	
		Born	Hard	Hard + SP	Hard	Hard + SP
91 GeV						
2 – 3	$480 \pm 140 \pm 110$	91	76	206	34	163
3 – 4	$240 \pm 60 \pm 50$	125	114	237	53	173
4 – 6	$110 \pm 30 \pm 10$	56	60	109	29	74
183 GeV						
2 – 3	$180 \pm 120 \pm 50$	55	51	68	25	42
3 – 4	$160 \pm 50 \pm 30$	67	70	86	34	49
4 – 6	$120 \pm 40 \pm 20$	53	70	85	35	47

Table 1: Comparison of the theoretical results to L3 data for $e^+e^- \rightarrow e^+e^- + \text{hadrons}$ with $E_{tag} > 30$ GeV, $30 \text{ mrad} < \theta_{tag} < 66 \text{ mrad}$. We show in the table $d\sigma/dY$ binned in Y obtained from experiment and the results of our calculation which take into account two-gluon exchange (Born approximation) perturbative pomeron (hard) and both perturbative and soft pomerons (hard + SP) for two different choices of scale of the α_s in impact factors and for e^+e^- CM energy 91 GeV and 183 GeV.

tion. We see that the contamination of the cross-section by soft pomeron is substantial. The data do also favour the smaller value of the scale of α_s . We also show in this table theoretical predictions in which the QCD pomeron was approximated by the two-gluon exchange contribution. We notice that throughout (almost) entire Y range, which is being probed at LEP the QCD pomeron is dominated by its two-gluon exchange part and that the effects of the BFKL enhancement are not visible. This is caused by the fact that in the region $Y < 4$ the two gluon exchange dominates the cross-sections $\sigma_{\gamma^*\gamma^*}^{ij}$ (see Fig. 2b) and that the BFKL enhancement is delayed to higher values of Y . We can notice onset of this enhancement in the last bin $4 < \Delta Y < 6$ by it is still a very weak effect. We conclude that the energies which are accessible at LEP are insufficient for probing the BFKL enhancement. This is due to the fact that the subleading effects delay the onset of the power-law BFKL behaviour of the cross-sections $\sigma_{\gamma^*\gamma^*}^{ij}$ to higher energies than those which are probed at LEP.

In Tab. 2 we show results of our estimate for the cross-section for the process $e^+e^- \rightarrow$

$\theta_{min} - \theta_{max}$	$\sigma(e^+e^- \rightarrow e^+e^- + hadrons)$ [fb]			Events / year
	Born	Hard	Full (LS)	Full (LS)
10–20	134	365	450	9000
20–30	16	41	46	920
30–40	3.5	8	9	180
40–50	1.1	2.3	2.5	50
50–70	0.6	1.1	1.3	26
30–70	5.2	11	13	260

Table 2: Predictions for TESLA at e^+e^- energy equal to 500 GeV. Cross-sections for $e^+e^- \rightarrow e^+e^- + hadrons$ with tagged electrons $E_{tag} > 30\text{GeV}$, $y_i > 0.1$, $2.5 \text{ GeV}^2 < Q_i^2 < 300 \text{ GeV}^2$, $2 < \ln[W^2/(Q_1Q_2)] < 10$, $\theta_{min} < \theta_{tag} < \theta_{max}$. Results of the calculation with the low scale of α_s in impact factors: two-gluon exchange (Born approximation), hard and full (hard+soft) contributions and the expected number of events per year, assuming the integrated luminosity per year to be $\mathcal{L} = 20\text{fb}^{-1}$.

$e^+e^- + hadrons$ with tagged e^+e^- in the final state for the total CM energy of the e^+e^- system equal to 500 GeV. We can see that in this very high energy region the QCD pomeron dominates over the soft pomeron contribution even for very low tagging angles. These cross-sections are also bigger by about a factor equal to 2–3 than the two-gluon exchange “background”.

Different configurations of the virtual photon polarizations contribute to the QCD pomeron part of the cross-section for the process $e^+e^- \rightarrow e^+e^- + hadrons$ with the following approximate relative normalizations: $(TT) : (TL + LT) : (LL) = 9 : 6 : 1$. This means that the transversely polarized virtual photons alone give about 60% of the QCD pomeron part of the cross-section.

To sum up we have estimated the total $\gamma^*\gamma^*$ cross-section and its impact on the cross-section of the process $e^+e^- \rightarrow e^+e^- + hadrons$ with tagged e^+e^- in the final state for LEP energies and for the energy range which may become accesible in TESLA and in other future e^+e^- linear colliders. We based our calculations on the QCD pomeron exchange generated by the BFKL equation (21) with the subleading effects which follow from the consistency constraint (20). We have also included the “soft” pomeron term which gives important contribution at moderately large values of Q^2 and W^2 . The subleading effects in the BFKL equation significantly reduce the QCD pomeron intercept and the magnitude

of the corresponding cross-sections. The total $\gamma^*\gamma^*$ cross-section and the cross-section of the process $e^+e^- \rightarrow e^+e^- + \text{hadrons}$ with tagged e^+e^- in the final state are smaller than those corresponding to the LO BFKL equation. For sufficiently high energies however they are significantly bigger than the cross-sections which would follow from the two-gluon exchange mechanism. We confronted our theoretical predictions with recent experimental results from LEP obtaining fairly reasonable agreement with the data. We find that the BFKL effects should become clearly visible for energies which can become accessible in future linear colliders.

Acknowledgments

We thank Albert De Roeck for his interest in this work and useful discussions. This research was partially supported by the Polish State Committee for Scientific Research (KBN) grants 2 P03B 184 10, 2 P03B 89 13, 2 P03B 084 14 and by the EU Fourth Framework Programme ‘Training and Mobility of Researchers’, Network ‘Quantum Chromodynamics and the Deep Structure of Elementary Particles’, contract FMRX–CT98–0194.

References

- [1] S.J. Brodsky, F. Hautmann, D.A. Soper, Phys. Rev. **D56** (1997) 6957; Phys. Rev. Lett. **78** (1997) 803 (Erratum-ibid. **79** (1997) 3544).
- [2] J. Bartels, A. De Roeck, H. Lotter, Phys. Lett. **B389** (1996) 742; J. Bartels, A. De Roeck, C. Ewerz, H. Lotter, hep-ph/9710500.
- [3] A. Białas, W. Czyż, W. Florkowski, Eur. Phys. J. **C2** (1998) 683; W. Florkowski, Acta Phys. Polon. **28** (1997) 2673; A. Donnachie, H.G. Dosch, M. Rueter, Phys. Rev. **D59** (1999) 74011; M. Boonekamp et al. hep-ph/9812523.
- [4] E.A. Kuraev, L.N. Lipatov and V.S. Fadin, Zh. Eksp. Teor. Fiz. **72** (1977) 373 (Sov. Phys. JETP **45** (1977) 199); Ya. Ya. Balitzkij and L.N. Lipatov, Yad. Fiz. **28** (1978) 1597 (Sov. J. Nucl. Phys. **28** (1978) 822); J.B. Bronzan and R.L. Sugar, Phys. Rev. **D17** (1978) 585; T. Jaroszewicz, Acta. Phys. Polon. **B11** (1980) 965; L.N. Lipatov, in “Perturbative QCD”, edited by A.H. Mueller, (World Scientific, Singapore, 1989), p. 441.
- [5] L.N. Gribov, E.M. Levin and M.G. Ryskin, Phys. Rep. **100** (1983) 1.

- [6] M. Ciafaloni, G. Camici, Phys. Lett. **B386** (1996) 341; *ibid.* **B412** (1997) 396; Erratum – *ibid.* **B417** (1998) 390; hep-ph/9803389; M. Ciafaloni, hep-ph/9709390; V.S. Fadin, M.I. Kotskii, R. Fiore, Phys. Lett. **B359** (1995) 181; V.S. Fadin, M.I. Kotskii, L.N. Lipatov, hep-ph/9704267; V.S. Fadin, R. Fiore, A. Flachi, M. Kotskii, Phys. Lett. **B422** (1998) 287; V.S. Fadin, L.N. Lipatov, hep-ph/9802290.
- [7] D.A. Ross, Phys. Lett. **B431** (1998) 161; G.P. Salam, JHEP **9807** (1998), 19; hep-ph/9806482; M. Ciafaloni, D. Colferai hep-ph/9812366; S.J. Brodsky et al. hep-ph/9901229; C.R. Schmidt hep-ph/9904368.
- [8] B. Andersson, G. Gustafson, H. Kharraziha, J. Samuelsson, Z. Phys. **C71** (1996) 613; J. Kwieciński, A.D. Martin, P.J. Sutton, Z. Phys. **C71** (1996) 585.
- [9] J.Kwieciński, A.D. Martin and A.M. Staśto, Phys. Rev. **D56** (1997) 3991.)
- [10] A. Donnachie and P.V. Landshoff, Phys. Lett. **B296** (1992) 227.
- [11] A. Donnachie and P.V. Landshoff, Z. Phys. **C61** (1994) 139.
- [12] L3 collaboration, (M. Acciari et al) CERN-EP-98-205 (1998).